Human Molecular Genetics, 1998, Vol. 7, No. 7 **1169–1178**

NB4S, a member of the TBC1 domain family of genes, is truncated as a result of a constitutional t(1;10)(p22;q21) chromosome translocation in a patient with stage 4S neuroblastoma

Terry Roberts, Olga Chernova and John K. Cowell*

Department of Neurosciences—NC30, Lerner Research Institute, Cleveland Clinic Foundation, 9500 Euclid Avenue, Cleveland, OH 44195, USA

Received February 27, 1998; Revised and Accepted April 24, 1998

Molecular cloning of the breakpoints of a t(1;10)(p22q21) constitutional translocation breakpoint in a patient with stage 4S neuroblastoma has identified two genes which are fused in-frame to generate a novel gene. The 1p22 gene, which we have called *NB4S*, encodes a 7.5 kb transcript with an 810 amino acid open reading frame and is expressed in a wide variety of tissues. *NB4S* has >88% homology with the mouse *EVI*-5 gene within the coding region and shows strong homology over a 200 amino acid region with TBC1 box motif genes involved in cell growth and differentiation. The C-teminal end of the protein contains a number of coiled coil domains, indicating a possible protein–protein binding function. The chromosome 10 breakpoint interrupts a novel transcript (*TRNG10*) which could only be detected in tumor cells. This transcript has no exon/intron structure or significant open reading frame, suggesting that it is a structural RNA which is transcribed but not translated. The chromosome rearrangement creates a fusion gene product which combines the TBC1 motif of *NB4S* with a polyadenylation signal from *TRNG10*, potentially generating a truncated protein with oncogenic properties.

INTRODUCTION

Constitutional chromosome rearrangements have been an important means of identifying genes that are involved in the predisposition to many human genetic disorders, including cancer. Translocations are generally more useful in positional cloning strategies, since the breakpoints usually interrupt the critical genes. Thus, even despite the handful of examples (1–3) where the breakpoints apparently map outside the causative gene, there is still a very realistic expectation that cloning the translocation breakpoints in these patients will reveal the gene responsible for the phenotype. We have used this strategy to investigate a constitutional chromosome translocation in a patient with stage 4S neuroblastoma.

Neuroblastoma is a malignancy arising from primitive neural crest cells that give rise to the adrenal medulla and the sympathetic nervous system. It is the most common extracranial solid tumor in children, accounting for 8–10% of all cases of pediatric neoplasms (4). Histopathologically neuroblastoma can be subclassified into several different groups (5), ranging from the most aggressive form, neuroblastoma, which is comprised entirely of immature neural precursor cells, to ganglioneuroma, which is comprised entirely of mature neural tissue. Ganglioneuroblastoma appears to lie between these two types and is comprised of both the primitive and mature elements in varying proportions. Whether these different manifestations of the disease represent discrete entities or form part of a series of progression stages is not clear. The most important prognostic factor for the patient with neuroblastoma is the extent of the tumor at the time of diagnosis and this has been classified into stages by various groups (6,7). Generally, the higher the stage is the more extensive is the tumor spread. Low stage (1 and 2) tumors do not show the metastatic spread seen in higher stage tumors (3 and 4). Within the spectrum of different presentations of neuroblastoma is a special stage known as stage 4S. This tumor type occurs mainly in children under the age of 1 year and is defined as a small stage 1 or 2 primary tumor but with a very particular pattern of metastatic disease. Metastatic deposits can be found in the skin, presenting as bluish lumps, in the bone marrow, where they form only a small proportion of the nucleated cells, and, most significantly, in the liver, with huge homogeneous involvement. The special feature of stage 4S neuroblastoma is that, despite the metastatic spread and the massive liver involvement, this tumor has the capacity to regress spontaneously. This observation led to the suggestion that stage 4S was a transient failure in differentiation (8). However, some stage 4S tumors, after an initial spontaneous regression, recur as a high grade malignancy and usually proceed to kill the patient (9). The mechanisms that allow for the early metastasis and huge expansion of immature neuroblasts, only to subsequently suffer spontaneous regression, are unknown, but characterizing the genetic events which allow this to occur will undoubtedly

*To whom correspondence should be addressed. Tel: +1 216 445 2688; Fax: +1 216 444 7927; Email: cowellj@cesmtp.ccf.org

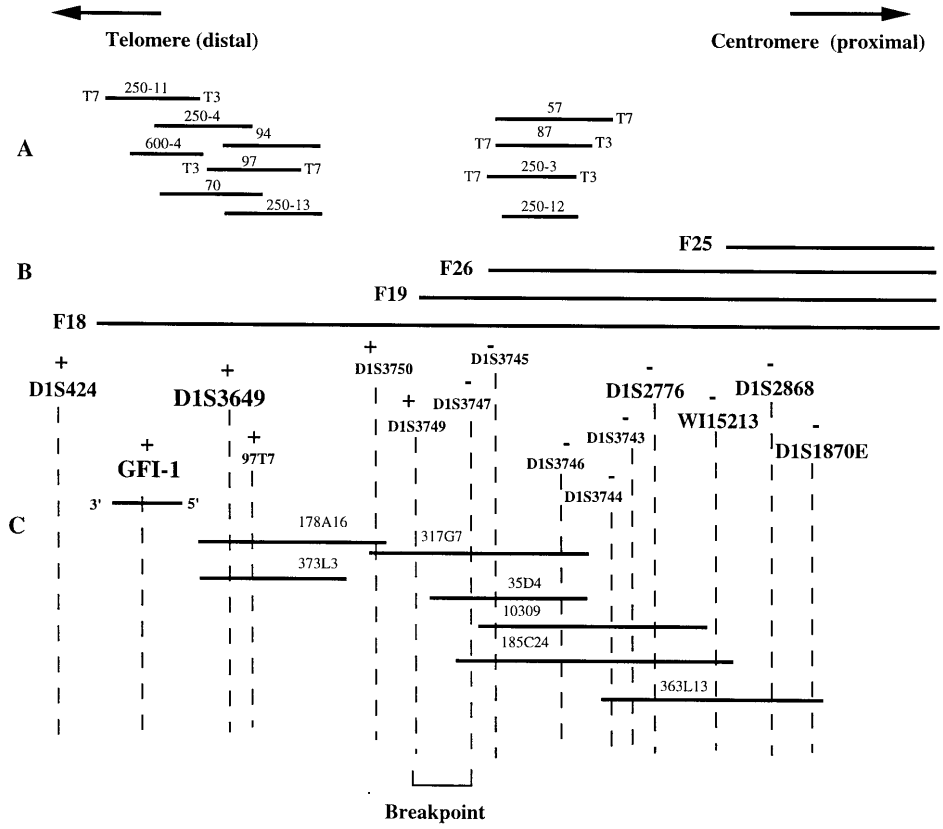

Figure 1. Diagramatic representation of the contig spanning the 1p22 breakpoint. In (**A**) the location of cosmids prepared from fragmented YAC F18 are shown relative to the four fragmented YACs shown in (**B**). Where the ends of cosmids were sequenced the orientation of the T7 and T3 ends are indicated. The BAC contig generated using the cosmid end clones and incorporating markers from the database is shown in (**C**). The ends of only one BAC, 317, were sequenced in order to confirm completion of the contig. Each of the markers on the linear map in (C) were tested for their presence or absence in the MWF72 somatic cell hybrid, which contains 1pter–1p22. Markers shown as (+) lay proximal to the breakpoint and markers shown as (–) lay distal to the breakpoint, which occurs in a 50 kb region between D1S3749 and D1S3747.

provide insights into the molecular mechanisms behind the phenomenon.

In our study of neuroblastoma we have previously described a patient with stage 4S disease and a constitutional, reciprocal, t(1;10)(p22;q21) chromosome translocation (10). This patient survived stage 4S neuroblastoma with no recurrence of the disease. To map the position of the chromosome translocation breakpoints we created somatic cell hybrids which had retained the translocated chromosomes but which had lost the normal homologs. These hybrids allowed us to map the exact position of the chromosomal breakpoints (10). We subsequently concentrated on the short arm of chromosome 1 because of the suggestion from tumor chromosome analysis that genes critical in the development of neuroblastoma were located there. Recently we described a YAC contig across the 1p22 region containing the breakpoint (11). Here we describe molecular cloning and characterization of the genes which are interrupted by this chromosome rearrangement.

RESULTS

Mapping the 1p22 breakpoint

Patient MW was treated successfully for stage 4S neuroblastoma and carries a constitutional chromosome translocation t(1;10)(p22;q21). Our previous analysis of the t(1;10) chromosome rearrangement using the MWF72 somatic cell hybrid, which contains the derivative chromosome 1 (10), demonstrated that the breakpoint lay within YAC 896B3 (11). When this YAC was fragmented and the resultant YACs analyzed by FISH, it was shown that a 650 kb YAC (F18) crossed the 1p22 breakpoint but an overlapping YAC, which was 400 kb long (F26), did not. Thus, the position of the breakpoint was sub-localized to a 200 kb region. At this time the closest flanking STS markers were D1S424 (distal) and D1S1870E (proximal). A summary of the map in this region is given in Figure 1.

From our FISH analysis, the 1p22 breakpoint was shown to lie in the region between the endpoints of YACs F26 and F19 (Fig. 1), although there were no markers in this region to define the position of the breakpoint further. In an attempt to build up a cosmid contig across the breakpoint region, DNA from the four fragmented YACs were subjected to Alu–PCR analysis. When the resulting band profile from these YACs was analyzed it was possible to identify Alu–PCR products which were absent from F25 but present in the other three fragmented YACs (data not shown). These PCR fragments provided probes in the proximal region of the breakpoint. Similarly, Alu–PCR products which were present only in F18 and not the other three YACs were also isolated. No specific Alu–PCR fragments were isolated from the interval between F26 and F19. A cosmid library was prepared

from the yeast cells carrying YAC F18 and probed with the inter-Alu probes which mapped proximal and distal to the breakpoint region. This resulted in the generation of two overlapping clusters of cosmids as shown in Figure 1. D1S424 was not present in cosmid 97 but the newly isolated STS 142D191 (D1S3649), described by Roberts *et al*. (11), which was derived from the end of YAC 142D1, was present and became the closest distal marker to the breakpoint. When the ends (T3 and T7) of selected cosmids were sequenced the relative overlap within this cluster was established. Similarly, the ends of two other cosmids, 87 and 250-3, shown by FISH to lie centromeric to the breakpoint (data not shown), were sequenced. PCR primers prepared from this sequence allowed the overlap within the second cluster to be established (Fig. 1). Using these new STS it was possible to demonstrate that the two cosmid clusters did not overlap. Rather than embarking on a cosmid walk at this point, and since we had now generated new probes within the breakpoint region, we decided to isolate BACs which spanned the gap between the two cosmid clusters.

Using the STS derived from the T7 end of cosmid 97 two BACs, 178 and 373, were isolated. In the same way BACs 317, 35, 103 and 185 were isolated with the STS derived from the T7 end of cosmid 87. The T3 end of cosmid 87 identified BAC 363 in addition to the others already isolated (Fig. 1). The various probes which we had generated within the breakpoint region were then assigned map positions within the BAC contig (Fig. 1). To determine whether BAC 317 overlapped with BACs 178 or 373, the distal end of this BAC was subcloned using vectorette PCR as described previously (11,12). Both ends of the subcloned fragment were sequenced. One end (D1S3750) was present in BAC 178 but not 373. The other end of this end clone (D1S3749) was present in BAC 317. Thus, we were able to demonstrate that the contig across the region was complete. All BACs were sized by pulsed field gel electrophoresis and the extents of the overlaps were determined by digesting independently with the restriction enzymes *Eco*RI, *Bam*HI and *Hin*dIII. At this time it was also possible to position several other markers, D1S2776, WI5213 and D1S2868, which had recently been assigned generally to this region, on the map. Importantly, using the MWF72 somatic cell hybrid (10) we were able to show that the 1p22 breakpoint lay between the T7 end of cosmid 250-3 (D1S3747) and D1S3749. Since both of the closest flanking markers were present in BAC 317, the breakpoint must lie in this region. FISH analysis confirmed that BAC 317 crossed the breakpoint (data not shown).

Cloning the gene, *NB4S*, interrupted by the 1p22 breakpoint

Our previous analysis of the YAC contig in 1p22 (11) identified a *Not*I fragment in F18, close to the position of the 1p22 breakpoint. Partial sequence analysis of a 9 kb *Eco*RI fragment containing this *Not*I site identified homology with the rat *Gfi*-1 gene (13). We subsequently cloned and sequenced this gene (13) and have now prepared STS from the 5′- (D1S3707E) and 3′-untranslated regions (D1S3708E) of human *Gfi*-1. Both ends of this gene were shown to lie distal to the 1p22 breakpoint in hybrid MWF 72 and were present in the contig containing cosmids 250-11 and 97, which allowed us to orientate this gene on the chromosome (Fig. 1). Neither end of this gene was shown to lie within BAC 178. All of these data excluded *Gfi*-1 from being interrupted by the translocation breakpoint. We next used the end clones isolated from our mapping effort to probe northern blots containing a variety of human tissues and demonstrated that D1S3649 identified a 7.5 kb transcript (data not shown) in a wide range of different tissues, including brain and adrenal. When the sequence data derived from this clone were used to search the genome databases, D1S3649 matched several anonymous ESTs as well as the IMAGE clone 324180 and the 3′-untranslated region of the mouse *EVI*-5 gene. We next used the mouse *EVI*-5 sequence to search the EST database and identified the IMAGE (human) clone 171671 (EST primer pair SGC 32492), which had a partial match to the 5′ coding region. This EST was located in BAC 317. Thus, the 3′-untranslated region of this gene lies on BAC 178 which, from FISH analysis, remains exclusively above the breakpoint and, since the 5′-end of the gene lies on BAC 317, which crosses the breakpoint, we can conclude that this gene is interrupted by the rearrangement. The mouse *EVI*-5 gene was so named because it was frequently the site of viral integration, although this observation gives no clue to its function. Because we have determined that this gene in humans is interrupted by a constitutional chromosome translocation in a patient with stage 4S neuroblastoma, we have called the human gene *NB4S*. Somatic cell hybrid analysis also confirmed that this gene is interrupted by the 1;10 translocation (see below).

Complete sequencing of the *NB4S* gene

Using the D1S3649 STS we could establish that *NB4S* was expressed in human liver and brain cDNA libraries using PCR. This probe identifies a 7.5 kb transcript which is present in virtually all tissue examined. Using this same PCR fragment to screen a liver cDNA library, 22 independent clones were isolated and the longest of these, L7, was 5.2 kb long (Fig. 2). Sequencing from both ends failed to detect the poly(A) signal or poly(A) tail. When a second clone, EST 324180 (Fig. 2), which was 1.5 kb long, was sequenced, the poly(A) tail was present at one end and the other end overlapped with clone L7 and included D1S3649 (Fig. 2). The L7 clone carried an open reading frame which extended to the very 5′-end of the clone and did not include the original EST (171671) from the 5′-end (see above). When the liver cDNA library was screened with this STS, a 1.3 kb clone was isolated which overlapped with clone L7 and EST 171671. The combined sequence, however, did not contain the initiation codon at the 5′-end of the gene. Using total RNA from adult brain we then used the 5′ RACE procedure and a nested set of primers to clone the 5′-end of the gene (NB5′), which contained the initiation codon (Fig. 2). We have now sequenced the entire *NB4S* gene (accession no. AF008915), which is 7.4 kb long and has an open reading frame of 810 amino acids.

NB4S homologies

BLASTN and BLASTP searches of the *NB4S* nucleotide sequence demonstrated an 88% homology with the mouse *EVI*-5 gene at both the nucleotide and protein levels over the coding region. However, the 3′-untranslated regions showed less homology, although in specific sub-regions the homology was up to 78%. The BLASTP searches also revealed significant homologies (Fig. 3) with the human *TRE*-2 oncogene, the mouse *TBC1* gene and a *Drosophila* gene, *pollux*. More recently, two other, as yet anonymous, genes (U49940 and 1061240) have been reported which show higher homologies with *NB4S* (Fig. 3). In each case, these homologies occurred over the 180 amino acid region

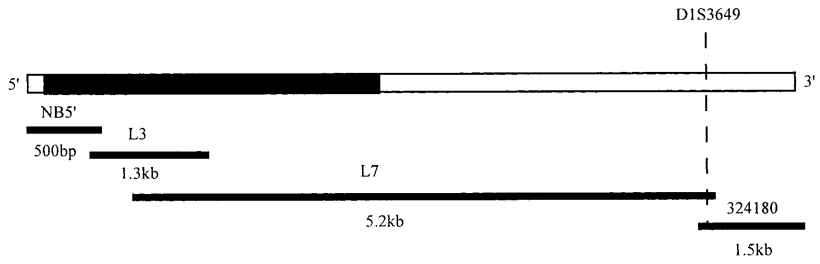

Figure 2. Relative overlap of the individual clones used to construct the *NB4S* gene. The dark box (above) represents the open reading frame. The positions of the ends of the individual cDNA clones are shown relative to the 7.4 kb gene. The 5′ clone, NB5′, was generated by RACE from fetal brain RNA.

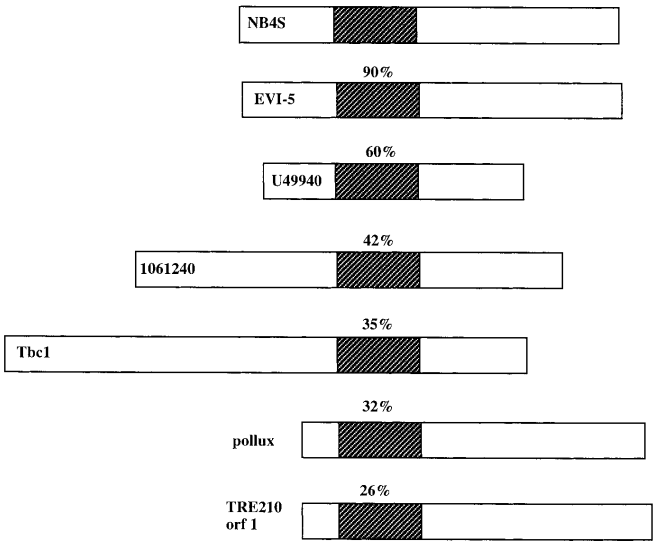

Figure 3. Comparison of the amino acid homologies between NB4S and other TBC1 box gene products. The homologies were confined exclusively to the TBC1 box and the extent of the homologies are indicated as percentages. Homologies were analyzed using the Mega-Align program from DNAStar and BLASTP searches.

(169–348) of all of these genes known as the TBC1 domain. Analysis of the C-terminal region of the *NB4S* gene product revealed a series of coiled coil domains (14) spanning amino acids 404–714.

Refining the position of the breakpoint within *NB4S*

In order to characterize the position of the breakpoint more accurately, a series of ESTs were designed throughout the length of the *NB4S* gene (Fig. 4) and tested against genomic DNA. Several of these ESTs produced PCR products which were the same size in both genomic DNA and the cDNA, demonstrating that they were intra-exonic. These primer pairs could also be used to analyze DNA from hybrid MWF72. The position of the newly generated ESTs (Table 1) were localized within the BAC and cosmid contig. The D1S3649 locus was present in both cosmid 97 and BAC 178 (Fig. 1). The T3 end of cosmid 97 was not present in BAC 178 but the T7 end was. Thus, since cosmid 97 is only 30 kb long, the 3′-end of *NB4S* must lie within 30 kb at the distal end of the contig. The 3′-untranslated and C-terminal end of the gene, spanning 5084 bp of the cDNA and defined by primer pairs UTR3, UTR2, UTR1 and C1 were all present on BAC 178. Coding (C) region 2 and C2.5 were present in BAC 317 and cosmid 43. C3 was also present in BAC 317 and cosmids 250-3 and 79. C4, C5 and EST 278249 were present in cosmids 79, 57 and 87 as well as BAC 317. EST NB4S2 was not in BAC 317 but in BACs 103, 185 and 363 as well as cosmid 57. This analysis of the distribution of ESTs demonstrated that the *NB4S* gene is spread over 270–300 kb of genomic sequence. Analysis of the MWF72 somatic cell hybrid using these ESTs (Fig. 4) places the breakpoint between C3 and C2, in the vicinity of C2.5 (1636–1718). Thus, the translocation breakpoint occurs within the coiled coil domain of the gene. Attempts to design EST primers from the cDNA sequence between C3 and C2.5 were not successful, suggesting that there are a series of small exons in this region.

Table 1. Summary of the nucleotide positions of the ESTs used to characterize the *NB4S* coding region (the GDB accession nos for the primer sequences for each of these primer pairs is also given)

EST	Position (bp)	GDB no.
UTR3	4861–51129	6900140
UTR2	3008–3186	6900138
UTR1	2447–2603	6900136
C1	2299–2436	6900134
C2	2037–1952	6900132
C2.5	1636–1718	6900147
C3	914–1026	6900130
C4	541–645	6900144
C5	349–468	6900142
EST278249	338–438	
NB4S2	141–250	6900148

3′ RACE to clone the fusion cDNA

As a result of our analysis of the BACs and the MWF72 hybrid using ESTs derived from within *NB4S*, we established that the breakpoint was close to EST marker C2.5. RT-PCR analysis of a lymphoblastoid cell line, 556A, which had been established from MW, demonstrated that the 5′-end (EST278) of *NB4S* was highly expressed, whereas the 3′-end (D1S3649) was not (data not shown). To identify the fusion partner gene on chromosome 10 we performed 3′ RACE using the C3 EST from *NB4S*, which was closest to breakpoint. As a result, a 1.2 kb fragment was

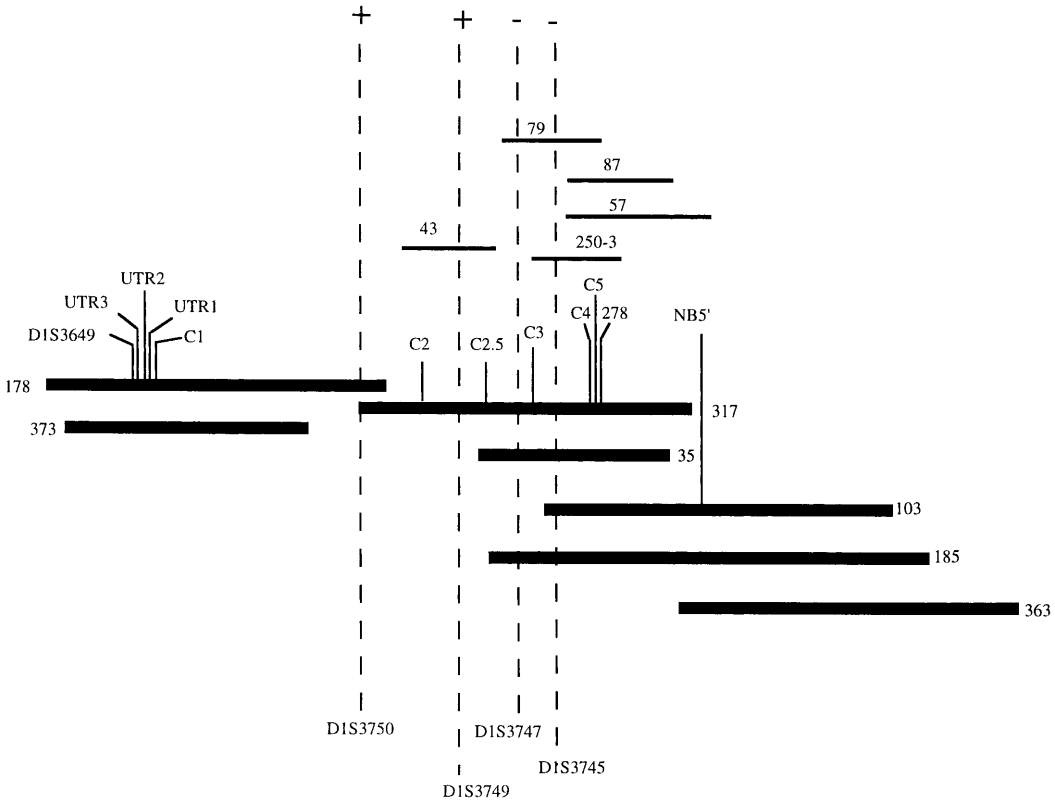

Figure 4. Location of ESTs used in the analysis of the *NB4S* gene. The position of the intra-exonic primer pairs (see Table 1) used to characterize the position of the breakpoint relative to the BACs in the contig (bold horizontal lines) and cosmids (thin lines above) are indicated. The position of the landmark STS flanking the breakpoint are shown below. The presence (+) or absence (–) of these STS in the MWF72 somatic cell hybrid are indicated at the top. The 1p22 breakpoint lies between EST C2.5 and C3.

amplified. Complete sequencing of this fragment identified the fusion point, at nt 1790 within *NB4S* (Fig. 5). The remaining 340 nt of the RACE product produces an in-frame fusion which contains a polyadenylation site, with a poly(A) tail 12 nt downstream. A pair of oligonucleotide primers (B and C; Fig. 5) were designed from within the non-*NB4S* sequence which amplifies a 100 bp fragment (D10S2493E). When a mono-chromosomal panel of somatic cell hybrids (15) was analyzed for the presence of this 100 bp fragment, a PCR product was seen only in hybrid 7628a (data not shown), which contains human chromosomes 10 and Y (16). The primer pair was then used to isolate a BAC clone, 20A12. FISH analysis using this BAC against chromosome spreads carrying the t(1;10) translocation showed that it hybridized to the q21 region of the normal copy of chromosome 10 and was also present on both derivative translocated chromosomes, demonstrating that it crosses the breakpoint (data not shown). When the genomic sequence around position 1790 was prepared from BAC 317, the position of the breakpoint was found to lie at an exon–intron boundary.

RT-PCR analysis of RNA from normal brain, liver, adrenal gland, thymus and the 556A lymphoblastoid cell line, using primers specific for the chromosome 10 sequence D10S2493E, produced an amplification product of the predicted size in all cases (Fig. 6). No PCR products were generated in samples where reverse transcriptase was excluded from the reaction, demonstrating the absence of contaminating DNA. In contrast, when the same RNAs were analyzed using primer pairs designed to amplify across the fusion point, a PCR fragment of the correct size was only seen in RNA obtained from the 556A lymphoblas-

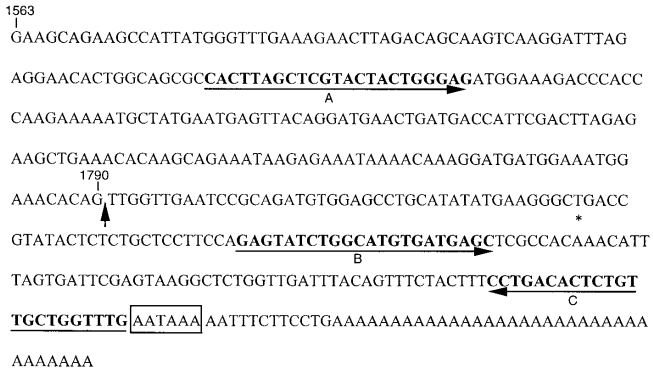

Figure 5. DNA sequence at the breakpoint junction fragment of the chimeric mRNA from patient MW beginning at nucleotide position 1563 in *NB4S*. The breakpoint (arrow) occurs at position 1790 in *NB4S* and 544 in *TRNG10*. The location of the primers, B and C, used to identify *TRNG10* mRNA are shown, as is the primer pair A and C, used to identify the junction fragment in the chimeric gene. As a result of this fusion an in-frame product is produced with a stop codon 43 bp downstream (indicated by *). The cryptic polyadenylation signal in the *TRNG10* gene lies adjacent to primer C (boxed), with the poly(A) tail in the chimeric gene being added 12 bp later.

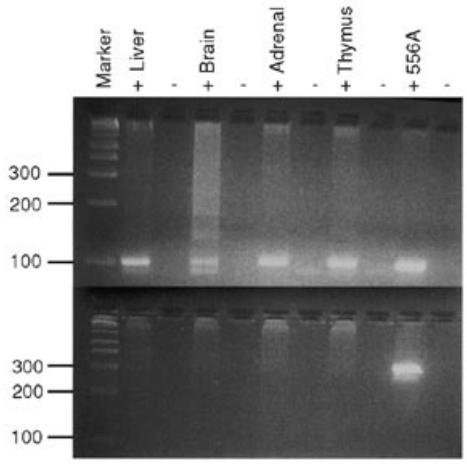

Figure 6. RT-PCR analysis of the *TRNG10* transcript. Analysis of RNA from a series of normal tissues (above) indicate that the 100 bp *TRNG*-specific fragment can be detected in reactions which included (+) reverse transcriptase but not in the same samples when reverse transcriptase was excluded (–). poly(A)$^+$ RNA was isolated from the lymphoblastoid cell line (556A) carrying the 1;10 translocation, which also shows the 100 bp fragment. When primers were used which cross the 1;10 translocation breakpoint (below) a PCR product of the predicted size (300 bp) is only generated from the cells carrying the rearrangement.

toid cell line (Fig. 6). in these experiments only poly(A)$^+$ RNA was used, further excluding the possibility of DNA contamination in the sample. These results indicated that the translocation breakpoint on chromosome 10 occurs within a transcribed sequence. We have named this gene translocation-related non-coding gene on chromosome 10 (*TRNG10*). Because the fusion product was not detected in normal tissues by RT-PCR, we conclude that the fusion gene is not a differentially spliced variant of the *NB4S* gene.

Cloning *TRNG10*

RT-PCR analysis indicated that *TRNG10* should be present in cDNA libraries from either brain, thymus, adrenal gland or liver. However, despite screening 10^6 clones from all of these libraries by hybridization, using both the 100 bp PCR product described above and a 3.5 kb *Eco*RI genomic fragment derived from BAC 20A12 (data not shown), no clones were identified. When northern blots containing RNA from multiple tissues were screened, no expression of *TRNG10* could be identified either. These results suggested that the RNA transcript from *TRNG10* was either not clonable or present at such low levels that it is not represented in the libraries tested from normal tissues. To establish whether this gene was expressed in tumor cells, we screened a northern blot containing RNA from a series of different cell lines (Fig. 7). A 2.8–3.0 kb transcript was identified in all cell lines except HeLa. We then screened 10^6 clones from the Jurkat human leukemia cDNA library and isolated two clones, 800 bp and 2.4 kb long. Subsequent screening of the cDNA libraries with the 2.4 kb cDNA did not identify additional clones. DNA sequence analysis of these two clones showed that the 800 bp clone was completely embedded within the 2.4 kb clone, at the point where the translocation event had occurred. Neither clone contained a poly(A) tail, although an adenylation signal was apparently present (see below). 3′ RACE was used to isolate the poly(A) region using RNA from human brain. A 500 bp PCR product was isolated which extended the sequence to the poly(A) tail. The complete *TRNG10* sequence (accession no. AF044579) is 2.8 kb long. Homology searches in the NCBI databases identified two different MER22 repeats located at positions 346–421 and 525–567. In the EST databases, matches to several entries were detected over these regions of MER repeats (17). Region 2620–2729 has 95% homology to the ALU repetitive element in both genomic and EST clones. The remainder of the sequence identified no other DNA sequence homology in the databases. Extensive sequence analysis identified only two potential open reading frames (ORFs). ORF1 was 85 amino acids long in the antisense direction between nt 391 and 648 and includes both MER22 repeats. ORF2, which encodes 82 amino acids, occurs at positions 2453–2701 on the sense strand and includes the ALU repeat. Several other very small ORFs were also found throughout the sequence. The highest GC content occurred at the beginning of the 5′-region. ORF1 and the ALU repeat had a GC content of 40–50%, but in the rest of the gene it was <35%. Using PCR primer pairs designed from different positions along the length of *TRNG10*, RT-PCR products could be generated in most normal RNA samples (data not shown), suggesting that *TRNG10* represents a transcribed gene rather than genomic DNA. When the genomic sequence corresponding to *TRNG10* was sequenced, no intron/exon structure could be detected.

Consequences of the 1;10 translocation

From DNA sequence analysis of both genes involved in the 1;10 translocation, it was possible to reconstruct the events which gave rise to the rearrangement. The 1p22 translocation breakpoint occurs within an intron of *NB4S* at a splice junction site and the 10q21 breakpoint occurs within the MER22 repeat of *TRNG10*. As a result, the ORF in the chimeric gene continues through the MER22 repeat at position 524 and reaches a stop codon immediately after the repeat sequence at nt 566 (Fig. 8). The sequence then continues within the *TRNG10* gene until the polyadenylation signal at nt 696, which causes premature termination of the fusion transcript. This translocation event results in the addition of a normally cryptic polyadenylation signal within *TRNG10* to the *NB4S* gene and this results in addition of a poly(A) tail and truncation of the *NB4S* gene at amino acid position 596 (accession no. AF042345). RT-PCR analysis of the 556A cell line demonstrates that only *NB4S*/*TRNG10* is transcribed as a result of this translocation, although the normal homologs of each of the genes on the normal chromosomes could also be detected.

DISCUSSION

We have characterized a novel, chimeric gene which is created as a result of a constitutional chromosome translocation in a patient with stage 4S neuroblastoma. This rearrangement results in the truncation of a potential oncogene through its fusion with a gene coding for a non-translated RNA. The fact that this constitutional chromosome translocation fuses two genes to create a novel chimeric gene, together with the fact that the patient develops a highly specific and particularly rare tumor, argues strongly for this rearrangement being causal in the development of the disease. Thus, we have identified two genes which are candidates

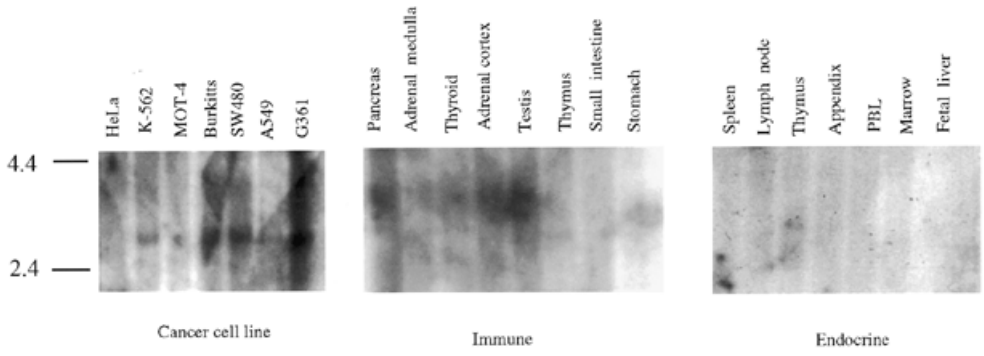

Figure 7. Northern blot analysis using the *TRNG10* cDNA. Expression of the 2.8 kb transcript was seen in all the cancer cell lines tested (left) except HeLa. No expression was detected in normal tissues, examples of which are shown from the immune (center) and endocrine (right) systems.

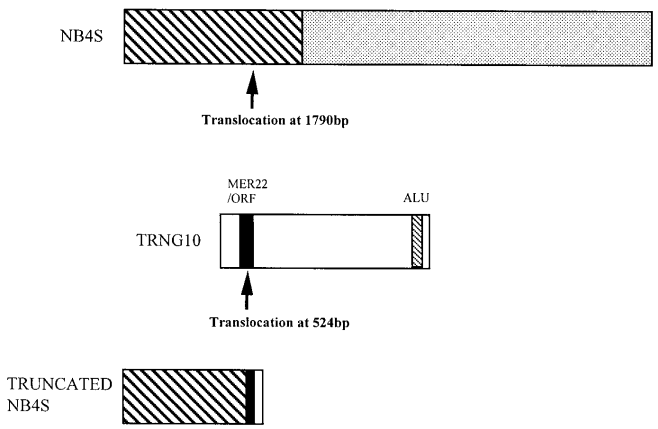

Figure 8. Summary of the composition of the chimeric *NB4S*/*TRNG10* gene. The mRNAs for both genes are shown diagramatically. The relative positions of the ORF (hatched) and UTR (shaded) in *NB4S* are shown. The positions of the MER22 and ALU repeats in *TRNG10* are also shown. The translocation breakpoint in *TRNG10* occurs in the MER22 repeat, which is fused in-frame to *NB4S*. Since a cryptic polyadenylation signal close to the translocation breakpoint is used by the chimeric gene, most of the *TRNG10* gene is not represented in the chimera.

for involvement in the development of stage 4S neuroblastoma. Whether this chimeric gene results in the generation of a stable oncogene or exhibits a dominant negative effect on the normal counterparts of the gene(s) is not yet clear. Unfortunately, the patient carrying this chromosome rearrangement was treated for her tumor 20 years ago and neither the patient nor her tumor are available for analysis.

The *NB4S* gene we have identified has some intriguing homologies which potentially implicate it in cell cycle control and/or differentiation. These homologies occur exclusively within the TBC1 domain motif, first identified in the mouse *TBC1* gene (18), which is presumed to have a role in regulating cell cycle control and differentiation. Other members of this group include the yeast *BUB2* and *cdc16* genes, which are also involved in regulation of the cell cycle (19,20). The other homology within the *NB4S* TBC1 domain is with the *TRE*-2 oncogene (21). This oncogene was originally isolated from NIH 3T3 cells transfected with Ewings sarcoma tumor DNA (21,22). The oncogene itself is made up of genomic DNA from human chromosomes 5, 18 and 17. The full-length gene consists of two ORFs and at least two alternatively spliced mRNAs called TRE210 and TRE213 (22). Only ORF1 from the TRE210 cDNA can cause cellular transformation. ORF2 has deubiquitinating activity, thereby allowing it to target proteins that are involved in cellular growth and differentiation for degradation by the ubiquitin-dependent pathway (23). It has been suggested that the transforming potential of ORF1 occurs by interfering with the normal product of the *TRE*-2 gene, thereby switching it off in some way such that the enzyme cannot degrade specific regulatory proteins that are involved in cellular proliferation. The homology between *NB4S* and the *TRE*-2 oncogene occurs within the oncogenic ORF1 (TBC1 box). This strongly suggests that *NB4S* has oncogenic potential as a result of structural rearrangement.

The normal *NB4S* gene is expressed ubiquitously (data not shown) and the product contains a coiled coil motif at the C-terminus of the protein. This motif implies a protein–protein or protein–DNA binding function. The translocation event in patient MW causes a truncation of NB4S which eliminates the coiled coil motif and presumably, therefore, the function of this motif. Coils are formed when right handed α-helices wrap around each other (24) and several different types of coil motifs have been identified to date, which include two, three and four stranded coils. Qian *et al.* (25), for example, showed that PKD1 interacts with PKD2 through a coiled coil motif and the interaction may regulate the activity of PKD2. Therefore, coil motifs seem to be involved in cellular protein–protein interactions, suggesting that NB4S may bind to other proteins within the cell and regulate their activity. Thus the 1;10 translocation may affect the ability of NB4S to interact with other components involved in the cell cycle, thereby leading to misregulation. In this respect *NB4S* may be functioning as a tumor suppressor gene and its disruption leads to oncogenic transformation through dominant negative interactions.

The highly specific expression profile of *TRNG10* also implicates it in tumorigenesis. So far, after screening a large number of commercially available northern blots containing poly(A) RNA, we have been unable to detect expression of this gene in any normal tissue. In contrast, a number of different tumorigenic cells lines show reasonable levels of expression. Since *TRNG10* could be detected at low levels in most normal RNA samples tested using RT-PCR, it appears that *TRNG10* is specifically activated, or more probably up-regulated or stabilized, in transformed cells. The stabilization theory is supported by our observations of the distribution of the transcript. Thus, although we could detect the *TRNG10* transcript in RNAs from different tissues, we could not isolate the gene from the

corresponding cDNA libraries, possibly suggesting that the *TRNG10* is highly unstable. Xu *et al*. (26) found that the first step in mRNA turnover is deadenylation, which is directed by RNA destabilization elements. The RNA first undergoes deadenylation, with very little degradation, whereafter the RNA is quickly degraded. It is possible that this transcript is missing in most cDNA libraries and lacks a poly(A) tail in other libraries because of its rapid turnover. Since stable transcripts were only found in a leukemia cDNA library and expression only occurs within transformed cell lines, this suggests that *TRNG10* could be a gene that is activated as a consequence of oncogenic transformation. A similar situation was reported by Askew *et al*. (27) for the non-coding *HIS*-1 gene. In this case retroviral insertion activated this gene and northern blot analysis demonstrated transcripts only in transformed cell lines and not normal tissues.

The fact that *TRNG10* could be detected in normal brain, liver, thymus, heart and adrenal glands by RT-PCR demonstrates that it is transcribed, but whether it is translated is not clear. Northern blot analysis showed a single full-length *TRNG10* transcript that is 2.8 kb long, the same length that is detected in genomic DNA. However, there were no characteristic gene motifs within the sequence, no significant ORF and no obvious exon/intron structure. It is possible, therefore, that *TRNG10* is one of the growing number of structural RNA genes that are transcribed but not translated. These include *NTT* (28), *IPW* (29), *H19* (30) and *Xist* (31). These genes vary in size from 2.2 (*IPW*) to 17 kb (*NTT*), contain no ORFs and frequently contain repeat motifs such as Alu, MER and Lines. They also have very specific expression patterns. Both *IPW* and *Xist* have very large exons and small introns. The *NTT* gene does not have an intron/exon structure at all and is apparently only expressed in activated human $CD4^+$ T cells. *TRNG10* could only be detected on northern blots containing RNA from tumor cells so far and does not have exon/intron structure either. The translocation occurs within the middle of *TRNG10* within a second MER22 repeat and causes a truncation of *NB4S*. RT-PCR analysis only detected expression of the unique fusion gene in the 556A lymphoblastoid cell line. Since only the *NB4S–TRNG10* fusion product could be detected but not the *TRNG10–NB4S* fusion product, it appears that *NB4S–TRNG10* is the oncogenic product generated by the 1;10 translocation. The RT-PCR analysis suggests that the truncated gene is overexpressed. The possibility that this truncation event results in stabilization of the truncated *NB4S* transcript is supported by the fact that the normal *NB4S* gene has 12 destabilizing sequences (AUUUA), as described by several authors (26,32), within the UTR which are lost as a result of the translocation. The truncated, chimeric gene lacks these motifs, which could make the transcript more stable, thereby contributing to its overexpression. There is evidence that repetitive elements can inactivate genes by splicing themselves into the coding regions (reviewed in ref. 33). These events usually result in truncation of the protein by introducing stop codons. Thus, the factor XI gene responsible for hemophilia B and the cholinesterase gene have been shown to be inactivated by insertion of Alu repeats into the coding region. In other cases, as we have seen in *NB4S*, the repetitive sequences can actually contribute extra codons to the host protein (33). In our case the rearranged *NB4S* coding region is extended by 42 bp derived from the MER22 repeat fused in-frame before the termination signal. This analogy suggests that *NB4S* is functionally inactivated as a result of the truncation. These various repetitive elements, as in *NB4S*, have also been shown to contribute cryptic poly(A) signals. Thus, as a result of insertion of an L1 element into the thymidylate synthase gene, for example, a poly(A) tail is added at the translational stop codon (34), with exclusion of the original 3′-untranslated region.

NB4S is the human homolog of the mouse *EVI*-5 gene (35). *EVI* (ectopic viral integration)-like genes are usually referred to as proto-oncogenes and they tend to be activated by chromosomal rearrangements. The *EVI*-1 gene in humans can be activated by chromosomal rearrangements involving either the 5′- or 3′-ends of the gene (36). The gene can also be activated as part of a fusion product. At present, it is not known whether proviral integration into the mouse *EVI*-5 gene, which occurs within the coiled coil motif, causes overexpression of the gene or whether integration causes loss of function of the gene through production of a truncated protein (35). The fact that the various homologs of *NB4S* are susceptible to activation/deactivation through chromosomal rearrangement strongly supports the role of the constitutional rearrangement in the development of neuroblastoma.

Another line of evidence strongly implicating *NB4S* in the development of neuroblastoma comes from transgenic studies in mice. Weiss *et al*. (37) used the tyrosine hydroxylase promoter, which is expressed in cells migrating off the neural crest during development, to overexpress the *MYCN* oncogene, which is amplified in many cases of neuroblastoma, in the neural crest cells of transgenic mice. When the karyotypes from these tumors were examined several chromosomes were consistently involved in rearrangements, suggesting sites of genes which contribute to the development of neuroblastoma. One of the most frequently rearranged chromosomes was mouse chromosome 5. We (13) and others (35,38–40) recently established a new region of synteny between human chromosome 1p22 and mouse chromosome 5. So far, the mouse genes that are part of this syntenic group are *GFI*-1 and *EVI*-5 and the region of mouse chromosome 5 that is frequently rearranged in *MYCN* neuroblastomas is exactly in the region of synteny (37).

Recent gene map data available from NCBI have mapped another member of the *TRE* family, *TRE*-17, within the consensus region on chromosome 17q11–12, frequently the site of chromosome translocation breakpoints in neuroblastoma. Thus, Laureys *et al*. (41) described a patient with stage 4 neuroblastoma who carried a t(1;17)(p36;q11–12) translocation. Other reports have described translocations involving breakpoints in chromosome 17p12 in tumors (42). Although the genes involved in these rearrangements have not been described, if they involve members of the *TRE* family this would provide a further indication that this family of genes plays a part in the development of neuroblastoma.

The genetic basis of neuroblastoma is proving to be very complex and, with the possible exception of *MYCN* (37), no candidate genes related to neuroblastoma tumorigenesis have been described to date. The *NB4S* and *TRNG10* genes, therefore, because of their constitutional rearrangement in a patient with stage 4S disease, offer exciting possibilities to study their role in tumorigenesis.

MATERIALS AND METHODS

Cosmid library construction

Yeast chromosomes were prepared in agarose plugs as described previously (11). Plugs were melted at 65°C for 15 min in 1× restriction enzyme buffer. The liquified plugs were then transferred to 37°C for 5 min. *Sau*IIIa (0.1 U; Gibco BRL) was added to the cooled liquified plugs and digestion allowed to proceed for 2–5 min. Digestion was then stopped by adding EDTA to a final

concentration of 25 mM and heating to 65°C for 15 min. The partially digested DNA was allowed to cool to room temperature and purified by phenol/chloroform extraction. The DNA was then precipitated with sodium acetate and ethanol and then resuspended to 0.5 µg/µl in sterile distilled water. The partially digested DNA was cloned into the Supercos vector (Stratagene) according to the manufacturer's protocol. Human clones were identified by hybridization using total human genomic DNA.

BAC library screening

BACs were isolated from the Research Genetics human BAC library, which was screened using STS markers according to the distributor's protocols. All clones were plated out onto LB agar plates containing 12.5 µg/ml chloramphenicol. Single clones were isolated and analyzed by colony PCR (11). Positive clones were then grown up in LB broth containing the appropriate antibiotic and DNA prepared using the alkali lysis procedure. BAC clones were sized by pulsed field gel electrophoresis after digestion with *Not*I using the following parameters; 1% agarose gel run at 6 V/cm for 17 h with a switch time of 6.7–13.5 s.

5′ and 3′ RACE

In order to clone the 5′-end of the *NB4S* gene, the 5′ RACE system and protocol from Gibco was followed. Aliquots of 2 µg total RNA from human brain (Clontech) were used for first round synthesis with the gene-specific primer GSP1 (5′-GTAACGATCTTGAA TGGAC-3′; nt 645–626). GSP2 (5′-TTCTACATGCGTTTTT-CTTC-3′, nt 468–448) was used in the first nested primer reaction and GSP3 (5′-CTAAGAAACCCTTCTTAACAAT-3′, nt 438–416) was used to generate the 5′-specific product.

For the isolation of sequences fused to the *NB4S* gene we carried out 3′ RACE on RNA extracted from the lymphoblastoid cell line 556A containing the constitutional translocation. Reverse transcription was performed using the 3′ RACE kit from Gibco. The first round of amplification was started with a GSP from the *NB4S* sequence nt 541–559 (5′-GCAGTGCACAAAGTATGCC-3′). A nested PCR reaction was performed using GSP2 at position nt 914–933 (5′-TCTTCCAGAGCTCTTTGTAC-3′) in order to generate a specific product. The 3′-end of the *TRNG10* sequence was also cloned using the 3′ RACE procedure. GSP1 at nt 2182–2222 (5′-CAATGCAAAGGTTGTCTGTCC-3′) was used in the first round amplification and GSP2 at nt 2215–2236 (5′-GACT-CATTTGTCTAAGTGGGCC-3′) was used to obtain a specific product. RACE products were cloned into the pGem-T vector (Promega) and transformed into JM109 competent cells (Promega). Clones were analyzed and sequenced using T7 and SP6 primers.

Alu–PCR for generation of specific differential probes

Fresh colonies from individual fragmented YAC clones were amplified directly in 100 µl PCR reaction buffer using the ALU III and ALU IV repeat primers (43). The amplification was carried out for 40 cycles using the following parameters, 94°C for 1 min, 55°C for 1 min and 72°C for 3 min. Following amplification, 50 µl of the reaction were run on a 1.5% low melting agarose gel until the bands were well separated. The banding patterns between different overlapping YAC clones were compared and bands that were present exclusively in the larger clones allowed them to be mapped within the YAC. These bands were cut out of the gel for use as probes for hybridization. PCR reactions were repeated twice to confirm that the banding patterns were consistent. All ^{32}P-labeled probes were competed at 65°C for 15 min with human placental DNA at 2.5 µg/µl before hybridization.

PCR and RT-PCR

RNA was isolated using Trizol reagent. Samples of 1–2 µg total RNA or 500 ng mRNA were reverse transcribed using Superscript II (Gibco) and random hexamers (Promega). All PCRs were performed using Taq polymerase and the buffer supplied by Gibco with 0.2 mM dNTPs and 0.2 µm primers. PCR products were analyzed on 3% agarose gels.

ACKNOWLEDGEMENTS

We are grateful to the CCF core sequencing facility for their assistance. This work was supported by NIH grant RO1 NS35791 and the Rose-Ella Burkhardt Endowment Fund.

REFERENCES

1. Ton, C.C.T. *et al.* (1991) Positional cloning and characterization of a pairedbox- and homeobox-containing gene from the aniridia region. *Cell*, **67**, 1059–1074.
2. Foster, J.W. *et al.* (1994) Campomelic dysplasia and autosomal sex reversal caused by mutations in an SRY-related gene. *Nature*, **372**, 525–530.
3. Vortkamp, A., Gessler, M. and Grezschik, K.H. (1994) Gli3 zinc finger gene interrupted by translocations in Grieg syndrome families. *Nature*, **352**, 539–540.
4. Parkin, D.M., Stiller, C.A. and Diever, C.A. (1988) International incidence of childhood cancer. *Int. J. Cancer*, **42**, 511–552.
5. Woods, W.G., Tuchman, M., Bernstein, M.L., Leclerc, J.M., Brisson, L., Brodeur, G.M., Shimada, H., Hann, H.L. and Robison, L.L. (1992) Screening for neuroblastoma in North America. 2-year results from the Quebec Project. *Am. J. Pediat. Hematol. Oncol.*, **14**, 312–319.
6. Evans, A.E., D'Angio, G.J. and Randolph, J. A. (1971) Proposed staging for children with neuroblastoma. Children's cancer study group. *Cancer*, **27**, 374–378.
7. Brodeur, G.M. *et al.* (1988) International criteria for diagnosis, staging, and response to treatment of patients with neuroblastoma. *J. Clin. Oncol.*, **6**, 1874–1881.
8. D'Angio, G.J., Evans, A.E. and Koop, C.E. (1971) Special pattern of widespread neuroblastoma with a favourable prognosis. *Lancet*, **i**, 1046–1049.
9. Nakagawara, A., Sasazuki, T., Akiyama, H., Kawakami, K., Kuwano, A., Yokoyama, T. and Kume, K. (1990) N-*myc* oncogene and stage IV-S neuroblastoma. Preliminary observations on ten cases. *Cancer*, **65**, 1960–1967.
10. Mead, RS. and Cowell, J.K. (1995) Molecular characterisation of a t(1;10)(p22;q21) constitutional translocation from a patient with neuroblastoma. *Cancer Genet. Cytogenet.*, **81**, 151–157.
11. Roberts, T., Tchernova, O. and Cowell, J.K. (1998) Molecular characterisation of the 1p22 breakpoint region spanning the constitutional translocation breakpoint in a neuroblastoma patient with a t(1:10)(p22;q21) rearrangement. *Cancer Genet. Cytogenet.*, **100**, 10–20.
12. Hawthorn, L., Roberts, T., Verlind, E., Kooy, R.F. and Cowell, J.K. (1995) A yeast artificial chromosome contig that spans the RB1–D13S31 interval on human chromosome 13 and encompasses the frequently deleted region in B-cell chronic lymphocytic leukemia. *Genomics*, **30**, 425–430.
13. Roberts, T. and Cowell, J.K. (1997) Cloning of the human *Gfi*-1 gene and its mapping to chomosome region 1p22. *Oncogene*, **14**, 1003–1005.
14. Lupas, A., Van Dyke, M. and Stock, J. (1991) Predicting coiled coils from protein sequences. *Science*, **252**, 1162–1164.
15. Hawthorn, L. and Cowell, J.K. (1996) Regional assignment of EST sequences on human chromosome 13. *Cytogenet. Cell Genet.*, **72**, 72–77.
16. Kelsell, D.P., Rooke, L., Warne, D., Bouzyk, M., Cullin, L., Cox, S., West, L., Povy, S. and Spurr, N.K. (1995) Development of a panel of monochromosomal somatic cell hybrids for rapid gene mapping. *Annls Hum. Genet.*, **59**, 233–241.

17. Rubin, C.M., Leeflang, E.P., Rinehart, F.P, and Schmid, C.W. (1993) Paucity of novel short interspersed repetitive elements (SINE) families in human DNA and isolation of a novel MER repeat. *Genomics*, **18**, 322–328.
18. Richardson, P.M. and Zon, L.I. (1995) Molecular cloning of a cDNA with a novel domain present in the *tre*-2 oncogene and the yeast cycle regulators *BUB2* and *cdc16*. *Oncogene*, **11**, 1139–1148.
19. Fankhauser, C., Marks, J., Reymond, A. and Simanis, V. (1993) The *S.pombe cdc16* gene is required both for maintenance of p34cdc2 kinase activity and regulation of septum formation: a link between mitosis and cytokinesis. *EMBO J.*, **12**, 2697–26704.
20. Chang, F. and Nurse, P. (1993) Finishing the cell cycle: control of mitosis and cytokinesis in fission yeast. *Trends Genet.*, **9**, 333–335.
21. Nakamura, T., Hillova, J., Mariage-Samson, R. and Hill, M. (1988) A rearranged transforming gene, *tre*, is made up of human sequences derived from chromosome regions 5q, 17q, and 18q. *Oncogene Res.*, **3**, 449–455.
22. Nakamura, T., Jana, H., Mariage-Samson, R., Onno, M., Huebner, K., Cannizzaro, L.A., Boghosian-Sell, L., Croce, C.M. and Hill, M. (1992) A novel transcriptional unit of the *tre* oncogene widely expressed in human cancer cells. *Oncogene*, **7**, 733–741.
23. Papa, F.R. and Hochstrasser, M. (1993) The yeast DOA4 gene encodes a deubiquitinating enzyme related to a product of the human *tre*-2 oncogene. *Nature*, **366**, 313–319.
24. Wolf, E., Kim, P.S. and Berger, B. (1997) MultiCoil: a program for predicting two- and three-stranded coiled coils. *Protein Sci.*, **6**, 1179–1189.
25. Qian, F., Germino, F.J., Yiqiang, C., Zhang, X., Somlo, S. and Germino, G.G. (1997) PKD1 interacts with PKD2 through a probable coiled coil domain. *Nature Genet.*, **16**, 179–183.
26. Xu, N., Chen, C.Y. and Shyu, A.B. (1997) Modulation of the fate of cytoplasmic mRNA by AU-rich elements: key sequence features controlling mRMA deadenylation and decay. *Mol. Cell. Biol.*, **17**, 4611–4621.
27. Askew, D.S., Li, J. and Ihle, J.N. (1994) Retroviral insertions in the murine *His*-1 locus activates the expression of a novel RNA that lacks an extensive open reading frame. *Mol. Cell Biol.*, **14**, 1743–1751.
28. Liu, A.Y., Torchia, B.S., Migeon, B.R. and Siliciano, R.F. (1997) The human *NTT* gene: identification of a novel 17kb noncoding nuclear RNA expressed in activated CD4+ T cells. *Genomics*, **39**, 171–184.
29. Wevrick, R. and Francke, U. (1997) An imprinted mouse transcript homologus to the human imprinted in Prader–Willi syndrome (IPW) gene. *Hum. Mol. Genet.*, **6**, 325–332.
30. Pfeifer, K., Leighton, P.A. and Tilghman, S.M. (1996) The structural *H19* gene is required for transgene imprinting. *Proc. Natl Acad. Sci. USA*, **93**, 13876–13883.
31. Brockdorff, N., Ashworth, A., Kay, G.F., McCabe, V.M., Norris, D.P., Cooper, P.J., Swift, S. and Rastan, S. (1992) The product of the mouse *Xist* gene is a 15kb inactive X-specific transcript containing no ORF and located in the nucleus. *Cell*, **71**, 515–526.
32. Shaw, G. and Kamen, R. (1986) A conserved AU sequence from the 3′ untranslated region of GM-CSF mRNA mediates selective mRMA degradation. *Cell*, **46**, 659–667.
33. Makalowski, W., Mitchell, G.A. and Labuda, D. (1994) Alu sequences in the coding regions of mRNA: a source of protein variability. *Trends Genet.*, **10**, 188–193.
34. Harendza, C.J. and Johnson, L.F. (1990) Polyadenylylation signal of the mouse thymidylate synthase gene was created by insertion of an L1 repetitive element downstream of the open reading frame. *Proc. Natl Acad. Sci. USA*, **87**, 2531–2535.
35. Laio, X., Du, Y., Morse, H.C., Jenkins, N.A. and Copeland, N.G. (1997) Proviral integration at the *EVI5* locus disrupts a novel 90kDa protein with homology to the *tre*2 oncogene and cell cycle regulatory proteins. *Oncogene*, **14**, 1023–1029.
36. Fears, S., Mathieu, C., Zeleznik-Le, N., Huang, S. and Rowley, J.D. (1996) Intergenic splicing of *MDS1* and *Evi1* occurs in normal tissues as well as in myeloid leukemia and produces a new member of the PR domain family. *Proc. Natl Acad. Sci. USA*, **39**, 1642–1647.
37. Weiss, W.A., Aldape, K., Mohapatra, G., Feuerstein, B.G. and Bishop, J.M. (1997) Targeted expression of MYCN causes neuroblastoma in transgenic mice. *EMBO J.*, **16**, 2985–2995.
38. Bell, D.W. *et al.* (1995) Chromosomal localization of a gene, *GFI*, encoding a novel zinc finger protein reveals a new syntenic region between man and rodents. *Cytogenet. Cell Genet.*, **70**, 263–267.
39. Zornig, M., Schmidt, T., Karsunky, H., Grzeschiczek, A. and Moroy, T. (1996) Zinc finger gene *GFI*-1 cooperates with myc and pim-1 in T-cell lymphomagenesis by reducing the requirements for IL-2. *Oncogene*, **12**, 1789–1801.
40. Liao, X., Buchberg, A.M., Jenkins, N.A. and Copeland, N.G. (1995) *Evi*-5, a common site of retroviral integration in AKXD T-cell lymphomas, maps near *Gfi*-1 on mouse chromosome 5. *J. Virol.*, **69**, 7132–7137.
41. Laureys, G., Speleman, F., Versteeg, R., Van der Drift, P., Chan, A., Leroy, J., Francke, U., Opdenakker, G. and Van Roy, N. (1995) Constitutional translocation t(1;17)(p36.31–p36.13;q11.2–q12.1) in a neuroblastoma patient. Establishment of somatic cell hybrid and identification of PND/A12M2 on chromosome 1 and NF1/SCA7 on chromosome 17 as breakpoint flanking single copy markers. *Oncogene*, **10**, 1087–1093.
42. Van Roy, N., Cheng, N.C., Laureys, G., Opdenakker, G., Versteeg, R. and Speleman, F. (1995) Molecular cytogenetic analysis of 1;17 translocations in neuroblastoma. *Eur. J. Cancer*, **31A**, 530–535.
43. Ledbetter, S.A., Nelson, D.L., Warren, S.T. and Ledbetter, S.H. (1990) Rapid isolation of DNA probes within specific chromosome regions by interspersed repetitive sequence polymerase chain reaction. *Genomics*, **6**, 475–481.